Hindawi
Advances in Materials Science and Engineering
Volume 2019, Article ID 6954918, 7 pages
https://doi.org/10.1155/2019/6954918

Research Article

Effect of Grain Size and Film Thickness on the Thermoelectric Properties of Flexible Sb_2Te_3 Thin Films

Pornsiri Wanarattikan,[1] Piya Jitthammapirom,[2] Rachsak Sakdanuphab,[2] and Aparporn Sakulkalavek[3]

[1]*Faculty of Science and Technology, Huachiew Chalermprakiet University, Samut Prakarn 10540, Thailand*
[2]*College of Advanced Manufacturing Innovation, King Mongkut's Institute of Technology Ladkrabang, Chalongksrung Rd., Ladkrabang, Bangkok 10520, Thailand*
[3]*Faculty of Science, King Mongkut's Institute of Technology Ladkrabang, Chalongkrung Rd., Ladkrabang, Bangkok 10520, Thailand*

Correspondence should be addressed to Aparporn Sakulkalavek; aparporn.sa@kmitl.ac.th

Received 11 October 2018; Accepted 19 December 2018; Published 8 January 2019

Academic Editor: Guang-xing Liang

In this work, stoichiometric Sb_2Te_3 thin films with various thicknesses were deposited on a flexible substrate using RF magnetron sputtering. The grain size and thickness effects on the thermoelectric properties, such as the Seebeck coefficient (S), electrical conductivity (σ), power factor (PF), and thermal conductivity (k), were investigated. The results show that the grain size was directly related to film thickness. As the film thickness increased, the grain size also increased. The Seebeck coefficient and electrical conductivity corresponded to the grain size of the films. The mean free path of carriers increases as the grain size increases, resulting in a decrease in the Seebeck coefficient and increase in electrical conductivity. Electrical conductivity strongly affects the temperature dependence of PF which results in the highest value of 7.5×10^{-4} W/m·K^2 at 250°C for film thickness thicker than 1 μm. In the thermal conductivity mechanism, film thickness affects the dominance of phonons or carriers. For film thicknesses less than 1 μm, the behaviour of the phonons is dominant, while both are dominant for film thicknesses greater than 1 μm. Control of the grain size and film thickness is thus critical for controlling the performance of Sb_2Te_3 thin films.

1. Introduction

In recent decades, there has been extensive research on thermoelectric materials and devices [1, 2]. In general, the performance or properties of thermoelectric materials depends on the temperature gradient (ΔT) and the dimensionless figure of merit (ZT). The dimensionless figure of merit is defined as $ZT = S^2\sigma T/K$, where S is the Seebeck coefficient (V/K), σ is the electrical conductivity ($\Omega \cdot m^{-1}$), K is the thermal conductivity (W/m·K), and T is the absolute temperature (K). However, at the present, most thermoelectric devices are dependent on bulk material properties, limiting the ZT, partly because of the Wiedemann–Franz law, which relate it linearly to electrical and thermal conductivities. Nevertheless, low-dimensional structures can provide significantly higher ZTs. Two-dimensional (2D) thin film-based thermoelectric devices are lower dimensional than the three-dimensional bulk phase [3–5]. Currently, one of the most important research topics is the development of flexible thermoelectric devices for a wide variety of wearable and portable applications. Moreover, applying with various heat sources, they are quite effective [6, 7]. In this work, a polyimide substrate was chosen as a substrate due to its low thermal conductivity and high upper working temperature (up to 400°C).

Antimony telluride (Sb_2Te_3) is considered one of the best thermoelectric materials since it can achieve a relatively high figure of merit at room temperature [2, 8, 9]. Thin film deposition techniques, namely, coevaporation, pulsed laser deposition, magnetron sputtering, and electrodeposition, have already been used for fabricating Sb_2Te_3. From the literature, Fan et al. [10] and Chen et al. [11] studied the

effect of substrate temperature and annealing temperature on the thermoelectric property of sputtered Sb_2Te_3 thin films. The power factor was enhanced with an increase in substrate temperature and annealing at 400°C. Das and Soundararajan [12] have conducted a study on the thermoelectric and electrical properties of vacuum-evaporated Sb_2Te_3 thin films. The Seebeck coefficient and electrical resistivity as a function of temperature and film thickness were investigated. Both the Seebeck coefficient and electrical resistivity are linear functions of the reciprocal of film thickness. In addition, Park et al. [2] studied the strain- and grain size-dependent thermal conductivity of Sb_2Te_3 thin films prepared by RF magnetron sputtering and post-annealing treatment. The modified Callaway model approach was used to analyse how the grain size affects thermal transport in Sb_2Te_3 thin films. They suggested that control of grain size or strain strongly influences the development of high-performance TE devices. Hence, both grain size and thickness significantly contribute to the properties of thermal transport properties.

However, the effect of thickness on the thermoelectric property was not reported in the literature. Thus, this is the first study of the effects of film thickness and grain size on the temperature-dependent ZT value of Sb_2Te_3 thin films on flexible substrates. The suitable thickness of Sb_2Te_3 thin films for thermoelectric application was investigated. The stoichiometric Sb_2Te_3 thin films with various thicknesses were deposited on a flexible substrate using RF magnetron sputtering. The Seebeck coefficient and electrical conductivity as a function of temperature were measured from 30 to 250°C. The theoretical lattice thermal conductivity was calculated based on the modified Callaway model. The effect of electronic and lattice energies on thermal conductivity was investigated.

2. Materials and Methods

Sb_2Te_3 thin films were fabricated on a polyimide sheet (DuPont™ Kapton® polyimide), using a RF magnetron sputtering technique. The Sb_2Te_3 target material (Stanford Advanced Materials, USA; purity of 99.9%) was used to deposit the Sb_2Te_3 films. Before deposition, the vacuum system reduced the pressure to a base pressure of 3×10^{-6} mbar and presputtered for 10 minutes in order to get rid of contamination and oxide from the target surfaces. The sputtering conditions were maintained as follows: power of 45 W and working pressure of 1.2×10^{-2} mbar to ensure that the stoichiometric ratio of Sb : Te was 2 : 3. The details of these conditions were published in our previous work [9]. The Sb_2Te_3 films of various thicknesses were controlled by varying the sputtering time to 15, 30, 45, and 60 min.

The crystal structures of Sb_2Te_3 thin films with different thicknesses were analysed by grazing incidence X-ray diffraction (BrukerAXS : D8DISCOVER). The surface morphology and cross-sectional images were collected using a field-emission scanning electron microscope (FE-SEM JSM-7001F). Measurements of Seebeck coefficients and electrical conductivity were conducted by a DC four-terminal method (ZEM-3, ULVAC-RIKO) from 30 to 250°C. The effects of grain size and film thickness on the temperature-dependent thermal transport of Sb_2Te_3 thin films were investigated using theoretical modelling based on the Callaway theory [2, 13] and a modified phonon scattering mechanism proposed by Park et al. [2].

3. Results and Discussion

3.1. Microstructural Analysis. For characterization, samples A, B, C, and D represented deposited Sb_2Te_3 films at 15, 30, 45, and 60 min, respectively. Figure 1 shows the XRD spectra of Sb_2Te_3 thin films. The films exhibit amorphous phases and polycrystalline structures, depending on the film thickness. When the thickness of Sb_2Te_3 films is lower than 1.0 μm, films exhibit dominant amorphous phases, as seen in samples A and B. When thickness increases, the films become polycrystalline structures with a high-intensity peak, as seen in samples C and D. The XRD spectra for Sb_2Te_3 were compared with JCPDS cards no. 72-1990. For Sb_2Te_3 films, the diffraction angles were observed at 28.40° and 42.40° corresponding to the (015) and (0111) planes. The Sb_2Te_3 films at various thicknesses show a preferred orientation of (015), while crystallinity improves as thickness increases. The grain size (D) of the thin film was estimated from Scherrer's equation. The XRD analysis results are summarized in Table 1. The grain size of the thin film increased as film thickness increased.

The surface morphological and cross-sectional images of Sb_2Te_3 thin films prepared with various deposition times were investigated by FESEM, as shown in Figure 2. The surface morphological images clearly demonstrate that the films fabricated under different deposition times were morphologically different. Shorter sputtering time resulted in films with small grain size and smooth surface (sample A). The films had larger grain size and a rough surface with increased sputtering time (samples B, C, and D). For cross-sectional SEM images, the thicknesses of Sb_2Te_3 films were as follows: A, 384 nm; B, 770 nm; C, 1150 nm; and D, 1804 nm. The SEM images correspond to a different XRD spectrum, and the increase in crystallization leads to an increase in grain size roughness. The composition of films was determined by EDS. The elemental content of Te in all thin films was approximately 60%. This result indicated that the stoichiometric Sb : Te ratio of antimony telluride is confirmed as approximately 2 : 3.

3.2. Electrical and Thermal Transport Properties. According to a simple theory for nearly free electrons [14], the effect of measuring temperature and carrier concentration on the Seebeck coefficient (S) can be given by the following equation:

$$S = \frac{8\pi^2 k_B^2}{3eh^2} m^* T \left(\frac{\pi}{3n}\right)^{2/3} (1 + R), \quad (1)$$

where k_B and h are Boltzmann and Planck constants, respectively, m^*, n, and T are the effective mass of the carriers, carrier concentration, and absolute temperature, respectively, R is a function of scattering. Equation (1)

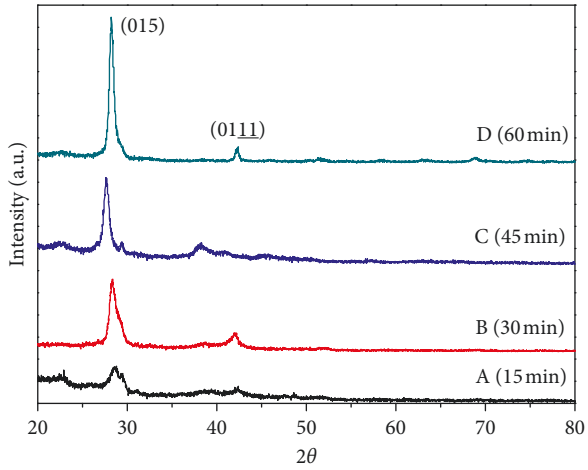

Figure 1: XRD spectra of Sb_2Te_3 thin films fabricated under different deposition times: 15, 30, 45, and 60 min.

Table 1: XRD analysis of Sb_2Te_3 thin films calculated from the (015) plane.

Sample	A	B	C	D
Film thickness, t (nm)	384	770	1150	1804
Grain size, D (nm)	5.25	10.80	14.12	23.80

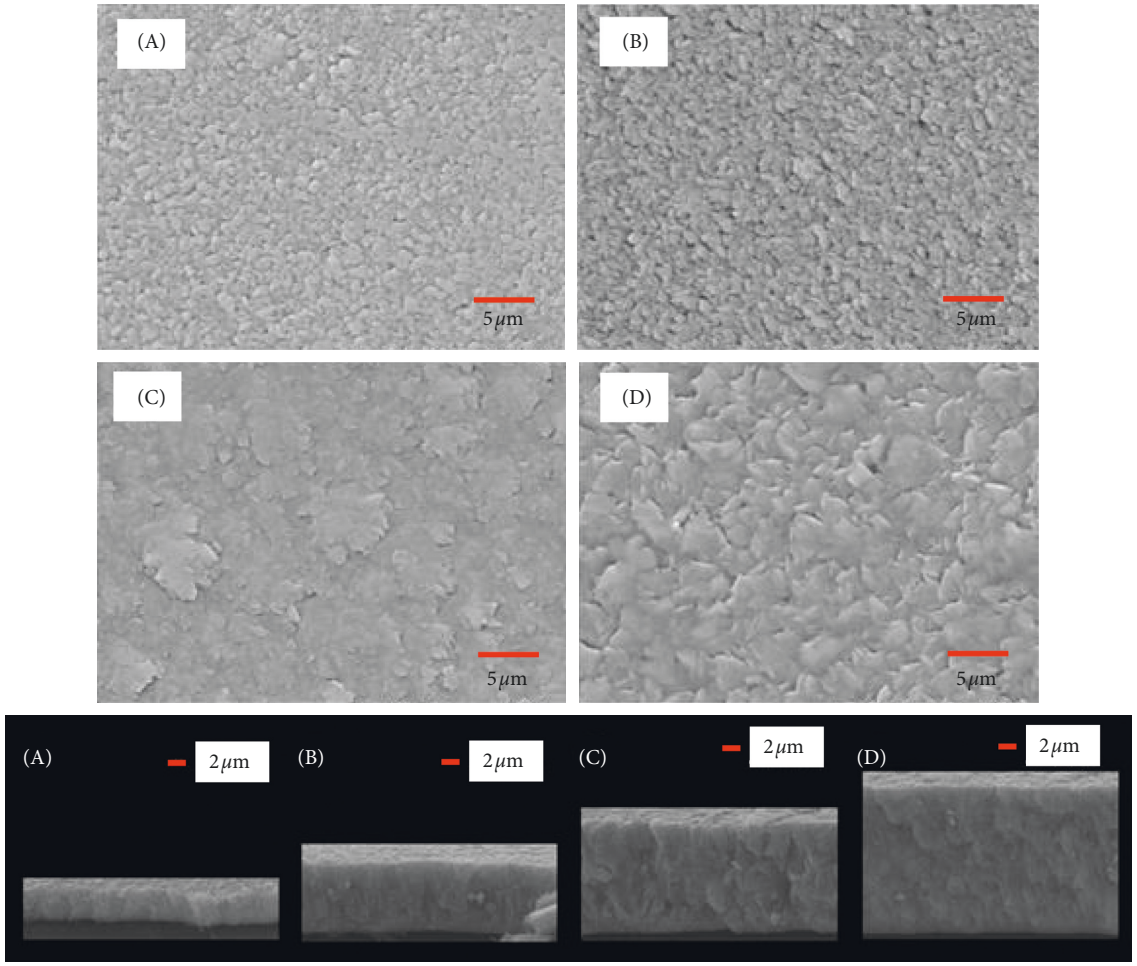

Figure 2: Surface morphological and cross-sectional images of Sb_2Te_3 thin films prepared by different deposition times at (A) 15, (B) 30, (C) 45, and (D) 60 min.

indicates that S is directly proportional to T and inversely proportional to n. In addition, the effects of film thickness and carrier mean free path on the Seebeck coefficient are as shown in the following equation:

$$S_F = S_B\left[1 - \frac{3(1-p)}{8}\frac{U}{1+U}\frac{\lambda_B}{t}\right], \quad (2)$$

where S_B is the Seebeck coefficient of the bulk material, p is the specularity parameter, λ_B is the mean free path of the carriers [13, 14], $U = \partial \ln \lambda_B / \partial \ln E$ is the exponent of the energy term for the mean free path of the form $\lambda_B = \lambda_0 E^p$. The exponent is 3/2 for impurity ion scattering, −1/2 for lattice acoustic scattering, and zero for optical phonon scattering, and so on; t is the thickness of the thin film. Equation (2) shows a direct proportion between Seebeck coefficient and thickness and inverse proportion between Seebeck coefficient and carrier mean free path.

According to Figure 3, the Seebeck coefficient (S) of Sb_2Te_3 films is a function of temperature, 50–250°C. The S values are positive over the entire temperature range which indicate hole conduction. Sample B exhibited the highest S value, and this S value was maintained at 210–230 μV/K. However, sample D shows the smallest S value, at approximately 165–180 μV/K. All films exhibited an identical behaviour of temperature-dependent on the S value. The S value of Sb_2Te_3 films was a function of temperature in the range of 50°C–200°C. The increase in the S value was due to the increase in temperature. However, as temperature increased, it not only affected the increase in S but also increased the carrier concentration. At temperatures above 200°C, the decrease in S was due to the increase in carrier concentration. For samples A and B, S increased with increasing film thickness. For samples C and D, the thickness was over 1 μm, and the grain size was greater than for samples A and B. We found that S decreased as the grain size increased, due to the increase in carrier mean free path or the decrease in carrier scattering. Zeng et al. [15] and Das and Ganesan [16] reported that λ_B decreases as the temperature increases was inversely proportional to temperature, due to increased lattice vibration or phonon scattering. In this work, we hypothesize that λ_B increases as the grain size increases, resulting in S values for films C and D that were lower than A and B.

To explain the thickness dependence of electrical conductivity, the logarithmic dependency of conductivity ($\ln\sigma$) on inverse temperature ($1000/T$) is displayed in Figure 4. All Sb_2Te_3 films exhibited linear characteristics that indicate the semiconductor behaviour of the film. In general, electrical conductivity depends on both carrier concentration (n) and mobility (μ), as shown in the following equation:

$$\sigma = n\mu q. \quad (3)$$

The carrier concentration in the Sb_2Te_3 thin film is dependent on the native antisite defects, Te_{Sb}, in the grain region, i.e., rich Te atoms occupying Sb lattice sites [17]. However, all samples had a similar stoichiometric ratio (Sb : Te = 2 : 3). The carrier may be not controlled by substitution defects. Conductivity increases with increasing crystallize size and carrier mobility. From the slope of the linear fit, the

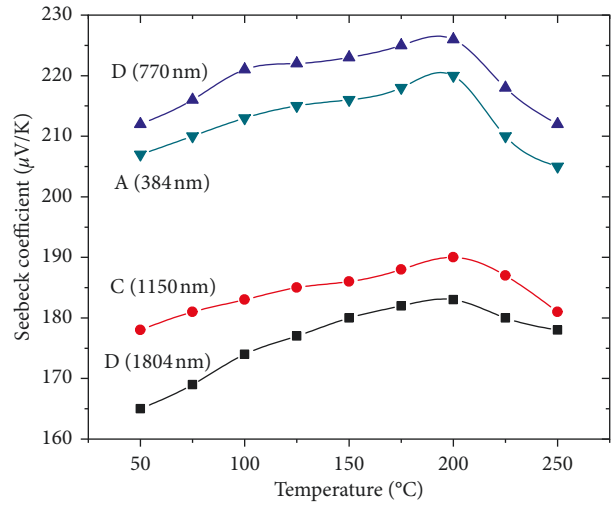

Figure 3: Variation in Seebeck coefficient as a function of temperature for Sb_2Te_3 films of different thicknesses.

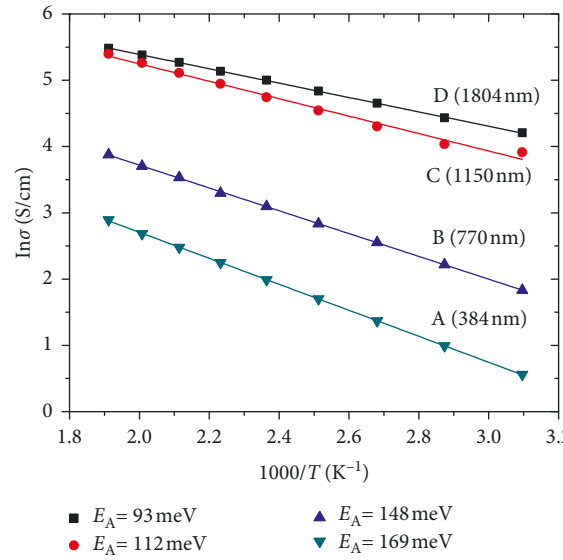

Figure 4: Plot of $\ln\sigma$ versus $1000/T$ for Sb_2Te_3 films of varying thicknesses.

activation energy for conduction in the films was calculated according to the relationship [16]:

$$\sigma = \sigma_0 \exp\left(-\frac{E_A}{k_B T}\right), \quad (4)$$

where σ_0 is the temperature-independent part of conductivity, E_A is the activation energy for conduction, k_B is the Boltzmann constant, and T is the absolute temperature. The calculated value E_A for samples A, B, C, and D was 169, 148, 112, and 93 meV, respectively. The activation energy for conduction decreases with increasing thickness. This result agrees with the reports from Zeng et al. [15] and Das and Ganesan [16]. These values do not correspond to the band gap of the material (200 meV) and should therefore be attributed to impurity levels [12]. The thickness dependence of E_A may be due to one effect or combined effects of

the following causes: (i) grain boundary barrier effect, (ii) quantum size effect, (iii) dislocation density, and (iv) deviation from the stoichiometric Sb/Te ratio [16]. In this work, the quantum size effect is negligible, since film thickness and grain size were relatively large and sputtering conditions were maintained to ensure that films had a stoichiometric Sb : Te ratio of 2 : 3. The major contribution might be due to the size of grains and dislocation density. The dislocation density (δ) is the length of the dislocation lines per unit volume of the crystal. It is expressed as

$$\delta = \frac{1}{D^2}. \tag{5}$$

The dislocation is an imperfection in the crystal which came into being during film growth [9], and dislocation density has a negative impact on electrical conductivity [13]. The δ values of films A, B, C, and D were 19.0×10^{15}, 8.6×10^{15}, 5.0×10^{15}, and $1.8 \times 10^{15}\ \mathrm{m}^{-2}$, respectively. We found that dislocation density was significantly correlated with larger grain size. As thickness increased, electrical conductivity increased due to the increase in grain size.

Figure 5 shows the power factor (PF) of Sb_2Te_3 films of varying thicknesses as a function of temperature. PF is a property of a material that generates energy from temperature difference. PF can be calculated by using the Seebeck coefficient and electrical conductivity ($S^2\sigma$) at a given temperature. The temperature dependence of PF is strongly influenced by electrical conductivity, resulting in the highest value of $7.5 \times 10^{-4}\ \mathrm{W/m{\cdot}K^2}$ at 250°C for sample D. However, only the value of PF was insufficient to evaluate the performance of a thermoelectric material, since this performance depends on both PF and thermal conductivity (k). In this work, the theoretical modelling of the thermal conductivity of the films was investigated using a phonon transport model, which is dependent on the relaxation time [13]. The expression for the expected lattice thermal conductivity (K_L) is given as follows [2, 13]:

$$K_L(T) = \frac{k_B}{2\pi^2 c}\left(\frac{k_B T}{\eta}\right)^3 \int_0^{\theta_D/T} \tau_c \frac{x^4 e^x}{(e^x - 1)^2}\, dx, \tag{6}$$

where k_B is the Boltzmann constant, η is the Planck constant, x is the dimensionless parameter with $x = \eta\omega/k_B T$, θ_D is the Debye temperature (θ_D = 160 K for Sb_2Te_3 [8]), and c is the speed of sound (2,900 m/s for Sb_2Te_3) [2]. Strain materials are widely studied in thermoelectrics, and the strain effects are known to affect thermal conductivity [1, 12]. Moreover, thermal transport has been investigated using numerical simulations, which show that thermal conductivity increases with increasing compressive strain and decreases with increasing tensile strain [18, 19]. However, Takashiri et al. [1] reported that the thermal conductivity of bismuth antimony telluride thin films depends on nanosize effects rather than the strain effect. In this work, the strain effect is negligible. Under relaxation time approximation, Park et al. [2] modified the scattering mechanism of the phonons from Callaway's initial suggestion and incorporated various scattering mechanisms which include dislocation, point defects, phonon-phonon scattering, and boundary scattering from the grain and thickness effect. Therefore, the total modified phonon scattering rate (relaxation time, τ_c) was adapted to be

$$\tau_c^{-1} = \frac{c}{D} + \frac{c}{t} + A\omega^4 + B\omega^2 T \exp\left(-\frac{\theta_D}{3T}\right) + C\omega, \tag{7}$$

where D and t are the grain size and thickness of the films, respectively, as shown in Table 1. The coefficients A, B, and C are temperature-dependent fitting parameters. For the Sb_2Te_3 film, the fitting parameters A, B, and C were approximately $9.6 \times 10^{-43}\mathrm{S}^3$, $2.7 \times 10^{-17}\mathrm{S/K}$, and 8.2×10^{-5}, respectively [2, 8].

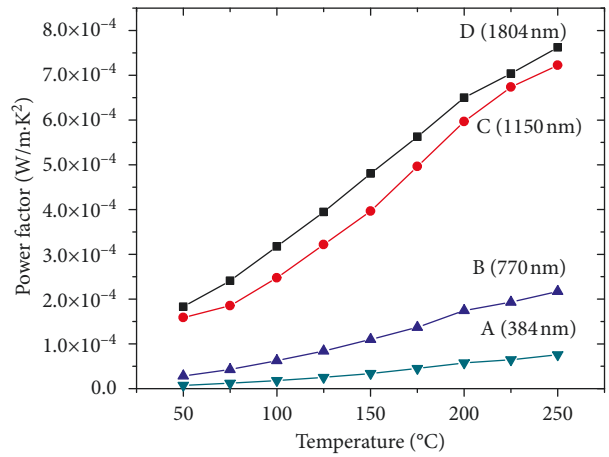

Figure 5: The variation of power factor as a function of temperature for Sb_2Te_3 films with varying thicknesses.

Figure 6 shows the theoretically calculated lattice thermal conductivity of Sb_2Te_3 thin films with varying thicknesses. The K_L of Sb_2Te_3 films decreased with increasing temperature, and this result indicated that phonon-phonon umklapp scattering was more significantly affected. In addition, the K_L of Sb_2Te_3 films increased with increasing film thickness and grain size, especially at low temperature (50°C). At high temperature, K_L tends to decrease, with a reduction in film thickness (grain size). According to Park et al. [2], grain size dominated the reduction of the K_L of antimony telluride thin film; here, grain size was determined to be approximately 88 to 129 nm, while K_L ranged from 0.61 to 1.08 W/m·K at temperature. In this work, we found that the grain size was approximately 7.25 to 20.80 nm, while K_L at room temperature was 0.37 to 0.48 W/m·K. This result indicated that the grain size effect caused the reduction of thermal conductivity of the Sb_2Te_3 thin film.

To estimate the electronic thermal conductivity, the Wiedemann–Franz law, $K_e = LT\sigma$, was calculated, where L is the Lorenz number ($2.45 \times 10^{-8}\ \mathrm{W\Omega/K^2}$) and T is the absolute temperature [2].

The electronic thermal conductivities from 50°C to 250°C for the various sample thicknesses are given in Figure 7. The K_e of samples B, C, and D increased with increasing temperature. This is thought to result from the enhancement of the carrier contribution to the thermal conductivity due to an increase in the carrier concentration with increasing

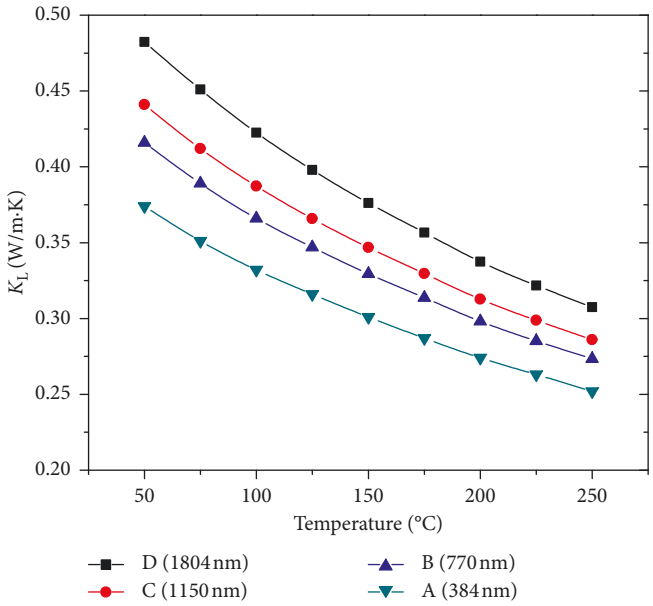

Figure 6: Theoretical calculation of lattice thermal conductivity for Sb_2Te_3 thin films as a function of measuring temperature.

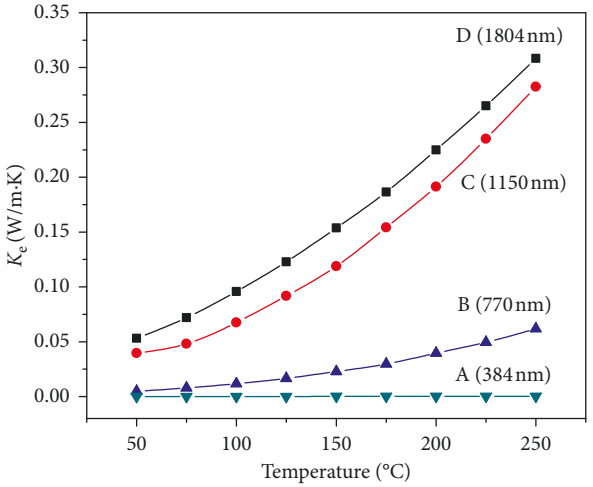

Figure 7: Electronic thermal conductivity of Sb_2Te_3 thin films as a function of measuring temperature.

temperature. In the case of sample A, K_e was approximately 5×10^{-5} W/m·K and slightly increased when the temperature surpassed 150°C. This was due to the small grain size, which creates scattering centres and obstructs the mobility of the carrier. Notably, the electronic thermal conductivity at 250°C for samples with film thicknesses over 1 μm (C and D) is approximate to the lattice thermal conductivity. The results may indicate that the mechanism of the thermal conductivity come from both the phonon and carrier. However, the film thickness affects the dominant phonon or carrier. For film thickness less than 1 μm, the behaviour of phonons is dominant, while both were dominant for film thicknesses greater than 1 μm. Figure 8 shows the temperature dependence of total thermal conductivity (K_{total}) for Sb_2Te_3 samples with various thicknesses. For samples A and B, K_{total} decreased with increasing temperature, and the contribution of K_e to K_{total} was quite small. For samples C and D, K_{total} decreased with increasing temperature below 100°C and increased with increasing temperature to 250°C.

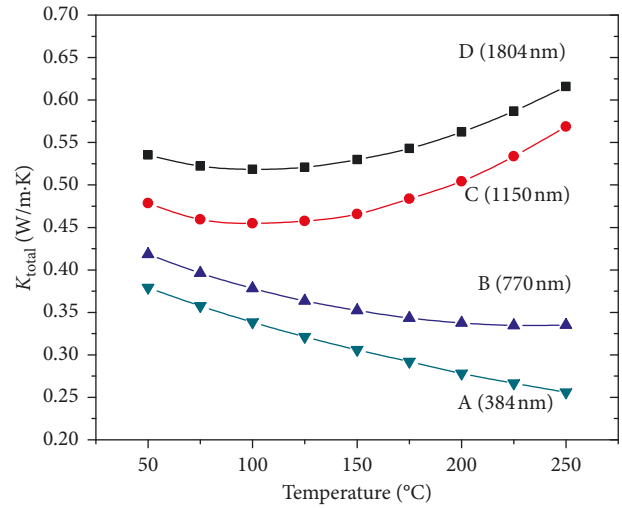

Figure 8: Calculation of total thermal conductivity for Sb_2Te_3 thin films as a function of measuring temperature.

Finally, the ZT of Sb_2Te_3 thin films with various thicknesses as a function of measuring temperature were calculated, as shown in Figure 9. The ZT value increases with increasing measuring temperature. This resulted from the enhancement of electrical conductivity. In the case of samples C and D, film thickness greater than 1 micron was effective in significantly improving thermoelectric performance. The highest value of ZT was obtained for samples C and D, with thicknesses of 1150 to 1804 nm. However, the electrical conductivity of samples A and B effectively decreased compared to samples C and D. From this result, the value of ZT of samples A and B was as small as samples C and D. Thus, the suitable thickness of Sb_2Te_3 thin films for thermoelectric application is approximately 1 μm.

4. Conclusions

In conclusion, the effects of grain size and film thickness on the thermoelectric properties of Sb_2Te_3 thin films were explained. The grain size of the films increased as film thickness increased and corresponded to the crystallinity. The films became polycrystalline structures when the thickness increased above 1 μm. The increase in the mean free path of carriers due to grain size enhanced the electrical conductivity and power factor of Sb_2Te_3 thin films. The highest PF of 7.5×10^{-4} W/m·K^2 at 250°C was obtained for the films with a thickness of 1.8 μm. The mechanism of thermal conductivity was explained by the Callaway model, which related to phonon or carrier scattering. For film thickness less than 1 μm, the phonon behaviourism is dominant, while both are dominant for film thickness above 1 μm. Finally, the calculated ZT suggested that a suitable

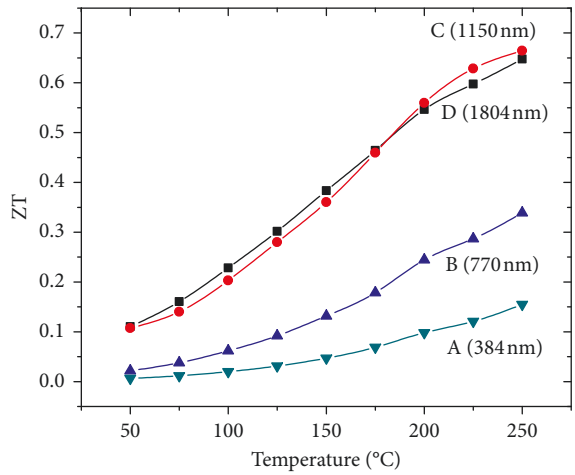

FIGURE 9: Calculation of ZT for Sb_2Te_3 thin films as a function of measuring temperature.

thickness for the Sb_2Te_3 thin film is approximately 1 μm for thermoelectric applications.

Data Availability

The data used to support the findings of this study are available from the corresponding author upon request.

Conflicts of Interest

The authors declare that there are no conflicts of interest regarding the publication of this paper.

Acknowledgments

The authors would like to acknowledge King Mongkut's Institute of Technology Ladkrabang for financial support.

References

[1] M. Takashiri, S. Tanaka, H. Hagino, and K. Miyazaki, "Strain and grain size effects on thermal transport in highly-oriented nanocrystalline bismuth antimony telluride thin films," *International Journal of Heat and Mass Transfer*, vol. 76, pp. 376–384, 2014.

[2] N.-W. Park, W.-Y. Lee, J.-E. Hong et al., "Effect of grain size on thermal transport in post-annealed antimony telluride thin films," *Nanoscale Research Letters*, vol. 10, no. 1, pp. 1–9, 2015.

[3] L. M. Goncalves, C. Couto, P. Alpuim, A. G. Rolo, F. Völklein, and J. H. Correia, "Optimization of thermoelectric properties on Bi_2Te_3 thin films deposited by thermal co-evaporation," *Thin Solid Films*, vol. 518, no. 10, pp. 2816–2821, 2010.

[4] H.-J. Lee, H. S. Park, S. Han, and J. Y. Kim, "Thermoelectric properties of n-type Bi-Te thin films with deposition conditions using RF magnetron co-sputtering," *Thermochimica Acta*, vol. 542, pp. 57–61, 2012.

[5] Q. Liqin, Z. Jian, C. Xuan, and A. Rajeev, "Electrochemical deposition of Bi_2Te_3-based thin films," *Journal of Physics and Chemistry of Solids*, vol. 71, no. 8, pp. 1131–1136, 2010.

[6] Z. Cao, E. Koukharenko, M. J. Tudor, R. N. Torah, and S. P. Beeby, "Flexible screen printed thermoelectric generator with enhanced processes and materials," *Sensors and Actuators A: Physical*, vol. 238, pp. 196–206, 2016.

[7] D. Madan, Z. Wang, P. K. Wright, and J. W. Evans, "Printed flexible thermoelectric generators for use on low levels of waste heat," *Applied Energy*, vol. 156, pp. 587–592, 2015.

[8] P. Lošták, Č. Drašar, J. Horák et al., "Transport coefficients and defect structure of $Sb_{2-x}Ag_xTe_3$ single crystals," *Journal of Physics and Chemistry of Solids*, vol. 67, no. 7, pp. 1457–1463, 2016.

[9] T. Khumtong, P. Sukwisute, A. Sakulkalavek, and R. Sakdanuphab, "Microstructure and electrical properties of antimony telluride thin films deposited by RF magnetron sputtering on flexible substrate using different sputtering pressures," *Journal of Electronic Materials*, vol. 46, no. 5, pp. 3166–3171, 2017.

[10] P. Fan, Z.-H. Zheng, G.-X. Liang, D.-P. Zhang, and X.-M. Cai, "Thermoelectric characterization of ion beam sputtered Sb_2Te_3 thin films," *Journal of Alloys and Compounds*, vol. 505, pp. 278–280, 2010.

[11] T. Chen, P. Fan, Z. Zheng et al., "Influence of substrate temperature on structural and thermoelectric properties of antimony telluride thin films fabricated by RF and DC cosputtering," *Journal of Electronic Materials*, vol. 41, no. 4, pp. 679–683, 2012.

[12] V. D. Das and N. Soundararajan, "Thermoelectric power and electrical resistivity of crystalline antimony telluride (Sb_2Te_3) thin films: temperature and size effects," *Journal of Applied Physics*, vol. 65, no. 6, pp. 2332–2341, 1989.

[13] J. R. Watling and D. J. Paul, "A study of the impact of dislocations on the thermoelectric properties of quantum wells in the Si/SiGe materials system," *Journal of Applied Physics*, vol. 110, no. 11, pp. 114508-1–114508-7, 2011.

[14] Z.-H. Zheng, P. Fan, G.-X. Liang, D.-P. Zhang, X.-M. Cai, and T.-B. Chen, "Annealing temperature influence on electrical properties of ion beam sputtered Bi_2Te_3 thin films," *Journal of Physics and Chemistry of Solids*, vol. 71, no. 12, pp. 1713–1716, 2010.

[15] Z. Zeng, P. Yang, and Z. Hu, "Temperature and size effects on electrical properties and thermoelectric power of Bismuth Telluride thin films deposited by co-sputtering," *Applied Surface Science*, vol. 268, pp. 472–476, 2013.

[16] V. D. Das and P. G. Ganesan, "Thickness and temperature effects on thermoelectric power and electrical resistivity of $(Bi0.25Sb0.75)_2Te_3$ thin films," *Materials Chemistry and Physics*, vol. 57, no. 1, pp. 57–66, 1998.

[17] B. Fang, Z. Zeng, X. Yan, and Z. Hu, "Effects of annealing on thermoelectric properties of Sb_2Te_3 thin films prepared by radio frequency magnetron sputtering," *Journal of Materials Science: Materials in Electronics*, vol. 24, no. 4, pp. 1105–1111, 2012.

[18] A. R. Abramson, C.-L. Tien, and A. Majumdar, "Interface and strain effects on the thermal conductivity of heterostructures: a molecular dynamics study," *Journal of Heat Transfer*, vol. 124, no. 5, pp. 963–970, 2002.

[19] R. C. Picu, T. Borca-Tasciuc, and M. C. Pavel, "Strain and size effects on heat transport in nanostructures," *Journal of Applied Physics*, vol. 93, no. 6, pp. 3535–3539, 2003.